J. Fluid Mech. (1994), *vol.* 267, *pp.* 299–324

The dispersion zone between fluids with different density and viscosity in a heterogeneous porous medium

By L. J. T. M. KEMPERS AND H. HAAS

Koninklijke/Shell Exploratie en Produktie Laboratorium, Volmerlaan 6, 2288 GD Rijswijk, The Netherlands

(Received 2 February 1993 and in revised form 2 November 1993)

A shock front in the concentration between two miscible fluids flowing through a porous medium becomes dispersed owing to the heterogeneous structure of the porous medium. If the fluids have equal viscosity and density and the heterogeneity of the porous medium is statistically homogeneous, the length of the dispersion zone between the fluids is known to increase as $(\beta X)^{\frac{1}{2}}$, where β is the dispersivity and X is the average displacement distance. At present the dispersivity is considered to be a property of only the porous medium. For the case where the fluids differ in density and/or in viscosity we have investigated the effect of the dynamics of the fluid flow on the magnitude of the dispersivity β and on the validity of the $X^{\frac{1}{2}}$ dependence of the dispersion zone's length. First, we measured the dispersivity in a 1.8 m long sandstone core with brine displacing water and with gas displacing oil. The measurements demonstrate that the dispersivity does indeed depend on the displacement velocity. Second, we monitored the expansion of the dispersion zone using detailed numerical simulations of the flow in a porous medium with statistically homogeneous heterogeneity. We found that the dispersion zone does grow as $X^{\frac{1}{2}}$ in the presence of a density contrast and a viscosity contrast, in spite of the nonlinearity of the governing equations. Third, we quantified the magnitude of the dispersivity by means of a random-walk model and tested the model against the experiments and the numerical simulations. Experiments, simulations and the model show that the dispersivity is strongly dependent on the displacement velocity in the conditionally stable flow regime. They also show that a nearly non-dispersive development of the shock front between the fluids occurs when gravity segregation dominates the dispersive effect of the porous medium. Even a very small difference in density, such as that between water and brine, can suppress the dispersivity significantly.

1. Introduction

When a fluid is displaced from a piece of porous material in a piston-like manner by the injection of another fluid that is miscible with the displaced fluid (so capillary effects are not present), the transition between the fluids in the effluent from the porous material is not sharp but gradual. Even if the fluid injection is so fast that molecular diffusion plays a negligible role in the mixing of the fluids in the porous material, the initial concentration shock front between the fluids still develops into a dispersed transition. This effect is partly due to the porous structure of the medium, which causes the fluid parcels to follow flow paths of different lengths. The most important contribution to the development of the concentration from an initially sharp shock

front to a dispersed transition zone comes from the heterogeneity of the porous medium at a lengthscale much larger than the pore size.

An often applied (and somewhat idealized) model of these heterogeneities in the porous medium is: (i) the permeability (or conductivity) of the porous material is random in space and statistically homogeneous, (ii) the correlation length of the permeability is small compared to the total size of the porous medium, and (iii) the distribution of the permeability values is log-normal. This type of heterogeneity causes a dispersion zone between the fluids; the length of this dispersion zone is known to increase as $(\beta X)^{\frac{1}{2}}$, where X is the average distance travelled by the fluids in the porous medium. The dispersivity β is solely a property of the porous medium, according to present knowledge. The hydrological theory of Gelhar & Axness (1983) has quantified β: $\beta = \lambda\sigma^2$, where λ is the correlation length of the permeability in the mean flow direction and σ is the standard deviation of the log-normal permeability distribution.

In this paper we show that significant deviations from the hydrological theory can occur. Our experiments, and our evaluation of experiments by others, demonstrate that the dispersion zone length not only depends on the distance travelled by the fluids and on properties of the porous medium, but also on the dynamics of the fluid flow. In particular, if the fluids differ in density and/or in viscosity, the dispersion zone length is also dependent on the displacement velocity, the density contrast, the viscosity contrast and the average permeability. For example, it is shown that a nearly non-dispersive development of the concentration shock front may occur due to gravity segregation of the fluids. It appears that, if the displacement velocity is low and the permeability is high, even a very small density difference, such as that between brine and water, may have a significant effect on the dispersion zone length.

The motivation for this work originates in several processes relevant to the oil and gas industry, such as oil recovery by injection of miscible gas. In many of these processes the displacing and displaced fluids differ significantly in density and in viscosity, which is not the case in hydrological processes for which the theory of Gelhar & Axness ($\beta = \lambda\sigma^2$) has been developed. For example, because the dispersion between the displaced fluid (oil) and displacing fluid (gas) requires more (expensive) gas to be injected than without dispersion, checking the relation for the dispersivity β may lead to significant cost reduction. It is demonstrated that a small density difference may also have an effect on the transition zone length; thus this work is of interest for hydrological processes too, particularly those which involve the invasion of seawater in a sweet water reservoir or the flow of pollutants in groundwater.

The objective of this work is to determine the length of the dispersion zone, and its growth as related to distance travelled, in the presence of a density contrast and a viscosity contrast between the displacing and displaced fluids. This is done for a piston-like displacement of a fluid by another miscible fluid. The paper is organized as follows. After a resumé of the present theory, we present three different investigations and integrate their results: (i) flooding experiments which demonstrate a dependence of the dispersion zone length on the displacement velocity, the viscosity contrast, the density contrast and the permeability; (ii) detailed numerical simulations of the flow of miscible fluids through a porous medium, in which the expansion of the dispersion zone is monitored to investigate the validity of the $X^{\frac{1}{2}}$ dependence of the dispersion zone's length when the fluids differ in density and in viscosity; (iii) a random-walk model that incorporates the dynamics of the fluid flow into the description of the dispersion zone; the model is validated by a comparison with the flooding experiments and the detailed numerical simulations.

Parts of the present paper are also presented in Kempers (1992) and in Kempers,

Haas & Groeneweg (1992). This work is restricted to stable displacements. It is part of a larger project on dispersion zones at Shell Research. An extension of this work to unstable displacements is presented in Kempers (1990) and in Kempers (1991). There it is shown that, under certain restrictions, the random-walk model can be applied to unstable displacements as well.

2. Theory

2.1. *Dispersed transition*

The flow at velocity $\boldsymbol{u}(\boldsymbol{r}, t)$ of two miscible, incompressible fluids in a porous medium is calculated from the mass balance equation, which yields a shock front in the concentration c of the displacing fluid:

$$\frac{\partial c}{\partial t} + \nabla \cdot (c\boldsymbol{u}) = 0; \tag{1}$$

from the transport equation for flow in a porous medium (Darcy's law):

$$\boldsymbol{u}\phi(\boldsymbol{r}) = -\frac{\boldsymbol{k}(\boldsymbol{r})}{\mu}(\nabla p + \rho g \nabla z), \tag{2}$$

where ϕ is the porosity, $\boldsymbol{k}$ the permeability tensor, μ the dynamic viscosity, ρ the density, g the gravitational acceleration, p the pressure, z the vertical coordinate; and from the continuity equation:

$$\nabla \cdot \boldsymbol{u} = 0. \tag{3}$$

Because detailed knowledge of irregular, short-distance variations in the permeability k is not normally available, average values for the permeability are used (Dagan 1989). However, the permeability variation causes irregular spatial variations in the flow velocity according to (2). A result is that two flowing miscible fluids develop a ragged interface. In laboratory experiments in which the production history of the fluids is measured, individual interface distortions cannot be detected but their sum is observed as a gradual transition between the fluids in the production history of the fluids. A way to describe these irregular flow variations is by a random-walk process superimposed on the average displacement velocity (Scheidegger 1957; Collins 1976); the above equations describing the flow of two miscible fluids are adapted by replacing the permeability by the effective permeability k_0, the porosity by the average porosity ϕ, and the concentration c by a volume-averaged value C, and by adding a diffusion-like term to equation (1) (Bear & Verruijt 1987). This results in

$$\frac{\partial C}{\partial t} + \nabla \cdot (C\boldsymbol{U}) = \nabla \cdot (\boldsymbol{K} \nabla C), \tag{4}$$

where $\boldsymbol{K}$ is the dispersion tensor and $\boldsymbol{U}$ is the average displacement velocity. Darcy's law and the continuity equation become

$$\boldsymbol{U}\phi = \frac{\boldsymbol{k}_0}{\mu}(\nabla p + \rho g \nabla z), \tag{5}$$

$$\nabla \cdot \boldsymbol{U} = 0. \tag{6}$$

Until now this has only been applied to cases in which the density ρ and viscosity μ do not depend on the concentration c.

In view of the restriction of this paper to piston-like displacements, the equations for one-dimensional, linear displacements are given (on the assumption that the dispersivity is independent of the space coordinates):

$$\frac{\partial C}{\partial t}+U\frac{\partial C}{\partial x}=K\frac{\partial^2 C}{\partial x^2}, \tag{7}$$

$$U\phi=-\frac{k_0}{\mu}\left[\frac{\partial p}{\partial x}+\rho g\sin\theta\right], \tag{8}$$

$$\frac{\partial U}{\partial x}=0, \tag{9}$$

where K is the longitudinal dispersion coefficient and θ the angle between the displacement direction and the horizontal.

2.2. *Magnitude of dispersivity*

The diffusion-like coefficient K in (7) is called the dispersion coefficient. The ratio K/U is called the dispersivity. The magnitude of K depends on the lengthscale as follows.

Microscopic dispersion at laboratory scale. The area of the flow domain is about 10^{-1} m. On this scale, microscopic heterogeneities occur due to pore geometry. Perkins & Johnston (1963) formulated the microscopic dispersion coefficient for fluids that have equal viscosity and equal density as

$$K=\frac{D}{F_R\phi}+0.5sd_gU \tag{10}$$

including as a condition the absence of Taylor dispersion (Taylor 1953): ($sd_gU/D<50$), where D is the molecular diffusion coefficient, d_g is the grain diameter and F_R is the formation resistivity factor. The second term in the dispersion coefficient ($0.5sd_gU$) is called the convective dispersion coefficient, denoted here as K_c. The inhomogeneity factor, s, is not precisely defined and must be measured.

Macroscopic dispersion at local scale. The area of the flow domain is about 10^0–10^3 m. On a local scale, heterogeneities occur within a reservoir layer on an areal correlation scale of the order of 10^{-1}–10^1 m and a vertical correlation scale of the order of 10^{-2}–10^0 m. At this local scale macroscopic dispersion dominates microscopic dispersion. Gelhar & Axness (1983) calculated the dispersion tensor based on stochastic spectral theory, assuming a statistically homogeneous geological layer with dimensions large compared with the correlation length of the permeability and for a frontal advance of several times the correlation length. They used a log-normal distribution of the permeability and an autocorrelation function for the log-permeability with an exponential decay with distance. The expression that they derived for the longitudinal dispersivity β_0 of an isotropic material when molecular diffusion is negligible is

$$\beta_0=K/U=\lambda\sigma^2. \tag{11}$$

(We have left out a correction factor $(1+\sigma^2/6)^{-2}$ in (11), which is minor for $\sigma<1$.) Since the theory of Gelhar & Axness is based on perturbation theory, a limitation to the theory is the restriction of the variance σ^2 of the log-normal distribution to a maximum of about 1. The theory can be applied widely, as shown by Gelhar (1986), who provided some data on variances and correlation lengths for various geological settings. Gelhar (1988) has shown for a field case that the expression $\lambda\sigma^2$ for the dispersivity is satisfactory beyond $\sigma=1$. A statistically homogeneous permeability distribution is of course a somewhat idealized type of local-scale heterogeneity, but it

seems to be a good approximation for many depositional settings; Gelhar (1986) gives many examples.

2.3. *Extent of dispersed transition*

With boundary and initial conditions $C = H(t)$ at $x = 0$ and $C = 0$ at $t = 0$ the solution to (7) for positive x and for $Ut \gg K/U$ is approximately (Bear & Verruijt 1987):

$$C = \tfrac{1}{2}\operatorname{erfc}\left(\frac{x-Ut}{2(Kt)^{\frac{1}{2}}}\right). \tag{12}$$

The dispersion zone is commonly defined as the zone in which the concentration, averaged over a cross-section perpendicular to the flow direction, varies from 10% to 90%. The length of the dispersion zone is then, with (12):

$$X_{10} - X_{90} = 3.62(Kt)^{\frac{1}{2}}, \tag{13}$$

where X_C is the distance travelled by a concentration C (C is denoted by percent). When molecular diffusion is neglected and the relations $\beta_0 = K/U$ and for the average distance travelled by the injectant, $X = Ut$, are substituted in (13), the dispersion zone length between fluids that have equal viscosity and equal density is

$$X_{10} - X_{90} = 3.62(\beta_0 X)^{\frac{1}{2}} \tag{14}$$

and is thus dependent on properties of the porous medium and the square root of the average distance travelled but it is independent of the displacement velocity.

Finally, the implicit restriction in the equations (12)–(14) (and in the rest of this work) is to flow that is stable. A flow with the lighter fluid on top of the heavier, and the less viscous fluid as the displacing agent is stable on condition that the displacement velocity does not exceed a critical velocity given by (e.g. Collins 1976; Stalkup 1983):

$$U_c = \frac{kg}{\phi}\left(\frac{\Delta\rho}{\Delta\mu}\right)\sin\theta. \tag{15}$$

The Δ in (15) refers to the overall difference between the displacing and displaced fluids. (To be certain that the mixing zone between the fluids is also internally stable, the minimum value of the derivative $\mathrm{d}\rho(c)/\mathrm{d}\mu(c)$ is to be used for the expression between brackets in (15).) In similar cases but with the more viscous fluid as the displacing agent, the displacement is unconditionally stable.

3. Observations from core-flooding experiments

Experimental evidence for the dependence of the dispersivity on the viscosity contrast and the density contrast was delivered in the early sixties, but has hardly been noted, probably because the measured dependence was weak in most cases. These experiments, which are discussed below, were conducted with the more viscous fluid as the displacing fluid. Our experiments, most of which were conducted with the less viscous fluid as the displacing fluid, show a stronger dependence.

In this paper we define a new quantity, the 'effective dispersivity', denoted by β, to account for the dependence of the dispersion zone length on the density, and on viscosity contrasts between the displacing and displaced fluids. At this stage the magnitude of β is not known; by definition it equals the dispersivity of the porous medium, β_0, in the absence of density and viscosity contrasts.

To obtain a coherent evaluation of all the reported experiments as well as our own, which were conducted with a wide variety of properties of fluids and porous media, we used a framework of dimensionless similarity groups. We derived the dimensionless similarity groups by bringing the basic equations (1)–(3), restricted to linear, miscible

displacements in two dimensions in a tilted porous medium, and the boundary and initial conditions, into a dimensionless form by dividing them by a characteristic value. The two most important similarity groups are

$$\text{mobility ratio} = \frac{\text{viscous force in fluid } P}{\text{viscous force in fluid } I}: \quad M = \frac{\mu_P}{\mu_I}; \tag{16}$$

$$\text{gravity number} = \frac{\text{gravity force}}{\text{viscous force}}: \quad N_G = \frac{k_0 g(\rho_P - \rho_I)\sin\theta}{\mu_P \phi U}. \tag{17}$$

In these definitions the injected fluid (displacing fluid) is denoted by subscript I and the produced fluid (displaced fluid) by subscript P.

3.1. *Measurements of effective dispersivity from the literature*

These experiments were conducted at mobility ratios smaller than one, and thus in the regime where the displacement is stable for all displacement velocities. The method of observation was to sample the effluent from the porous medium and measure the fractions of the displacing and displaced fluids in each sample. The expansion of the transition zone during its journey through the porous medium was not monitored; we assumed that the transition zone could be described by (12).

An increase of effective dispersivity with mobility ratio was experimentally shown by Brigham, Reed & Dew (1961). They found that in a glass pack placed in the horizontal position, dispersion is suppressed when the displacing fluid is less mobile than the displaced fluid. At a mobility ratio of 0.175 the dispersion was suppressed by a factor of 5 compared with the dispersion at a mobility ratio of 0.998. Because of the horizontal orientation of the glass pack, the gravity number N_G was 0 in his experiments. The trend observed is thus an increase in effective dispersivity with increasing mobility ratio (at $M < 1$ and $N_G = 0$).

Slobod & Howlett (1964) conducted 48 experiments in a core 1.22 m long, mounted vertically. Since Slobod & Howlett explored both the stable region and the unstable region, we have taken only those experiments that were stable both during the displacement and at rest (some of their experiments had the heavier fluid on top of the lighter fluid). The results are shown graphically in figure 1(*a*). (The data points with $N_G = 0$ are represented on the logarithmic N_G-scale as $N_G = 0.01$.) The figure shows that the experiments of Slobod & Howlett can be summarized as follows: effective dispersivity decreases with increasing gravity number, somewhere between $N_G = 0.1$ and $N_G = 1$ ($M < 1$).

Ben Salah (1965) conducted vertically upward displacements of pure water by a mixture of water and 45% wt glycerine. The mobility ratio was 0.21. Different glass bead packs were used; each pack was characterized by an average bead diameter. In each glass pack four or five displacements were conducted at different velocities. In some experiments, the displacement velocity was so high that Taylor dispersion must have played a role. Experiments with Taylor dispersion are characterized by a value greater than 1 for the ratio $K_c/25D$ (Perkins & Johnston 1963). For the evaluation of the trend with gravity number we have left out the experiments with a value greater than 0.9. The remaining experiments are shown in figure 1(*b*). The conclusion is that the experiments of Ben Salah demonstrate a small decrease in effective dispersivity with increasing gravity number at M of 0.21 and N_G between 0.2 and 10.

Giordano, Salter & Mohanty (1985) found suppression of dispersion with a decrease of the mobility ratio, in a few numerical simulations of miscible displacement in a reservoir with many local-scale permeability variations. They found that the profile of

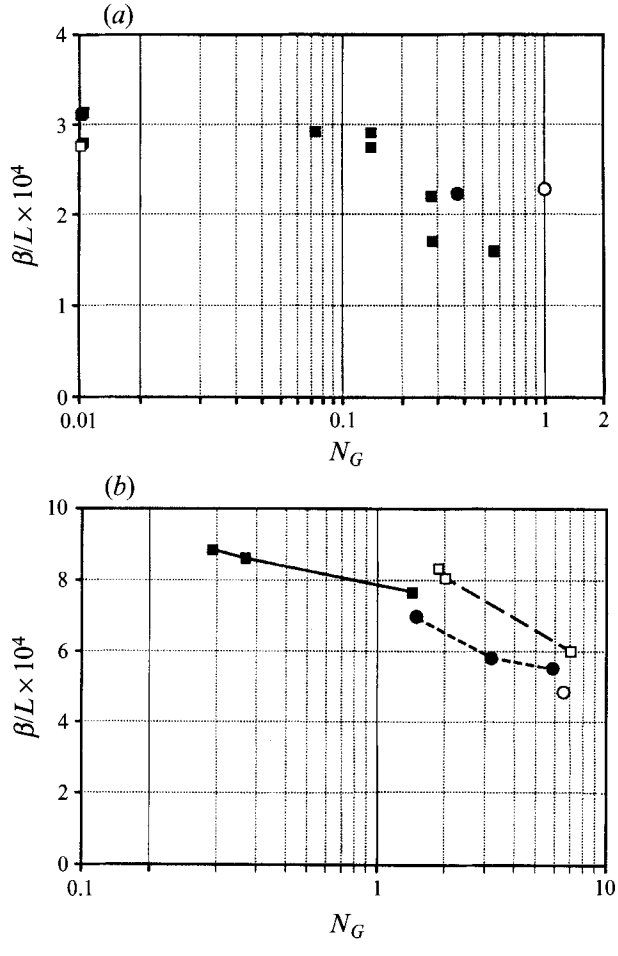

FIGURE 1. Evaluation of experiments reported in the literature: dimensionless effective dispersivity versus gravity number. (*a*) Slobod & Howlett (1964): ■, $M = 0.47$; □, $M = 0.437$; ●, $M = 0.374$; ○, $M = 2.275$. (*b*) Ben Salah (1965): ■, Sample 21; □, Sample 22; ●, Sample 23; ○, Sample 24.

the concentration of displacing fluid in the effluent was steepened when the mobility ratio was decreased from 1 in the first simulation run to 0.1 in the second run. Further decrease of the mobility ratio to 0.01 in a third run did not affect the effluent profile. Because gravity was not present in their simulation, the gravity number was zero. Brigham *et al.*'s finding is thus confirmed by the results of Giordano *et al.* Further, these authors demonstrated that a non-zero effective dispersivity remains at very small mobility ratio and $N_G = 0$.

Newberg & Foh (1988) conducted fast nitrogen/methane displacement tests in various cores with lengths limited to 15 cm. The experiments were conducted vertically in the upward direction. Since the tests with the lighter methane injected at the bottom to displace the heavier nitrogen could have been unstable at rest, we evaluated only the nitrogen-displacing-methane tests. In the paper the dispersion coefficients determined from the experiments are fitted by a nonlinear relation between dispersion coefficient and displacement velocity. However, the spread in the datapoints is too large to conclude that the datapoints cannot be matched by a linear relation. Therefore we reject the claim of the authors that their experiments, which were conducted at gravity

	Property	Value
L	length (m)	1.829
W	diameter (m)	0.051
d_p	average pore size (m)	28×10^{-6}
ϕ	porosity	
	water/brine	0.230
	gas/oil	0.242
F_R	formation resistivity factor	
	water/brine	13.8
	gas/oil	12.1
k	permeability (μm^2)	
	brine	0.45
	n-decane	0.62
σ	standard deviation of $\ln k$	0.17 ± 0.01
λ	correlation length of k (cm)	1.5 ± 0.5

TABLE 1. Data of Berea sandstone core

numbers below 0.3, demonstrate a dependence of the dispersivity on the density and viscosity contrast.

3.2. *Our experimental programme on effective dispersivity*

The objective of our experimental programme was to investigate the dependence of effective dispersivity on gravity number at mobility ratios larger than one (at which a displacement is stable only if the displacement velocity does not exceed the critical velocity U_c). The motivation for the experimental programme is to see whether the effective dispersivity is dependent on the displacement velocity at high displacement velocities (but below the critical velocity U_c), or whether it is independent of displacement velocity at high displacement velocities as demonstrated by the reported experiments conducted at $M < 1$.

The length of the core (in this case a Berea sandstone core) was 1.82 m. We selected such a long core because we could then carefully monitor the transition zone between the displacing and displaced fluids. Another reason for choosing a long core was to minimize the relative contribution of the dispersion in the inlet and outlet tubes of the equipment to the dispersion in the core. Table 1 lists the properties of the core.

To quantify the permeability variation of the Berea core we used a so-called mini-permeameter. This instrument forces air to flow from a thin tube that is pressed against the rock surface, through a part of the porous medium 0.5 cm in size. From a calibrated relationship between flow rate and pressure the permeability can be determined. The measurements, which were done at regular intervals of 1 cm, show spatial permeability variations (figure 2). The assumption that the distribution of the permeability values is log-normal is confirmed with the χ^2 test (with the level of significance of 80%; critical χ^2 value is 6.2). The auto-correlation function $R(x)$ of the permeability (figure 3) shows a rapid decrease at small x and is practically zero at x larger than a few centimetres. On the assumption that $R(x)$ has the form $\sigma^2 \exp(-|x|/\lambda)$, we determined $\lambda = 1.5 \pm 0.5$ cm and $\sigma = 0.17 \pm 0.01$. As a result, the dispersivity of the core ($\beta_0 = \lambda\sigma^2$) is $4.3 \pm 1.9 \times 10^{-4}$ m.

The transition zone between displacing and displaced fluids was continuously monitored by measuring the density of the effluent by means of a vibrating U-tube with an accuracy of 0.05%. To prevent fluid movement by thermal expansion, the core holder and fluid vessels were installed in a thermostatic cabinet. In all experiments the

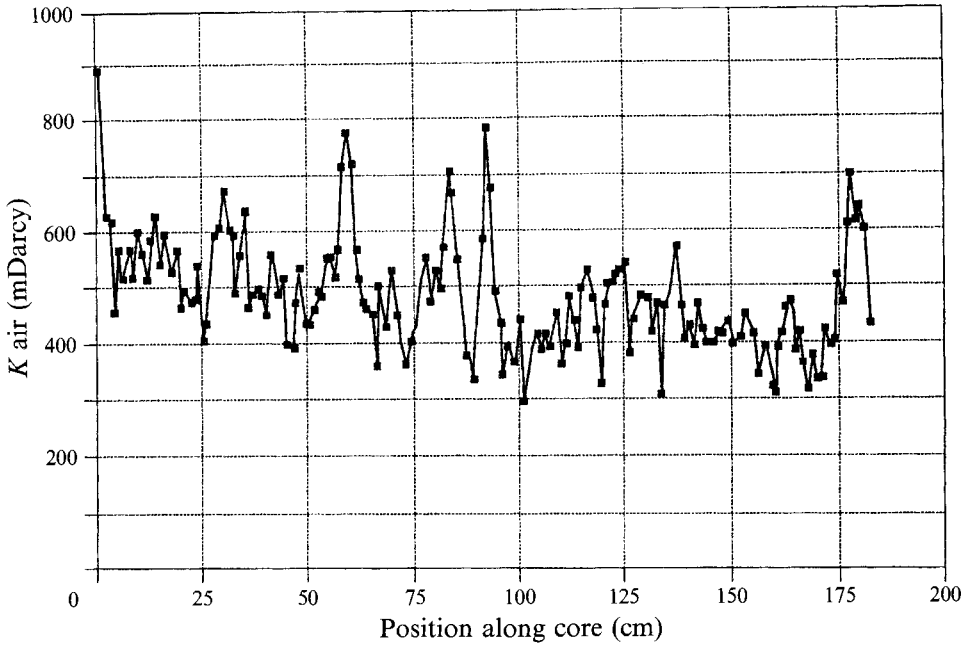

FIGURE 2. Air permeability along the Berea core measured with the mini-permeameter at 1 cm intervals.

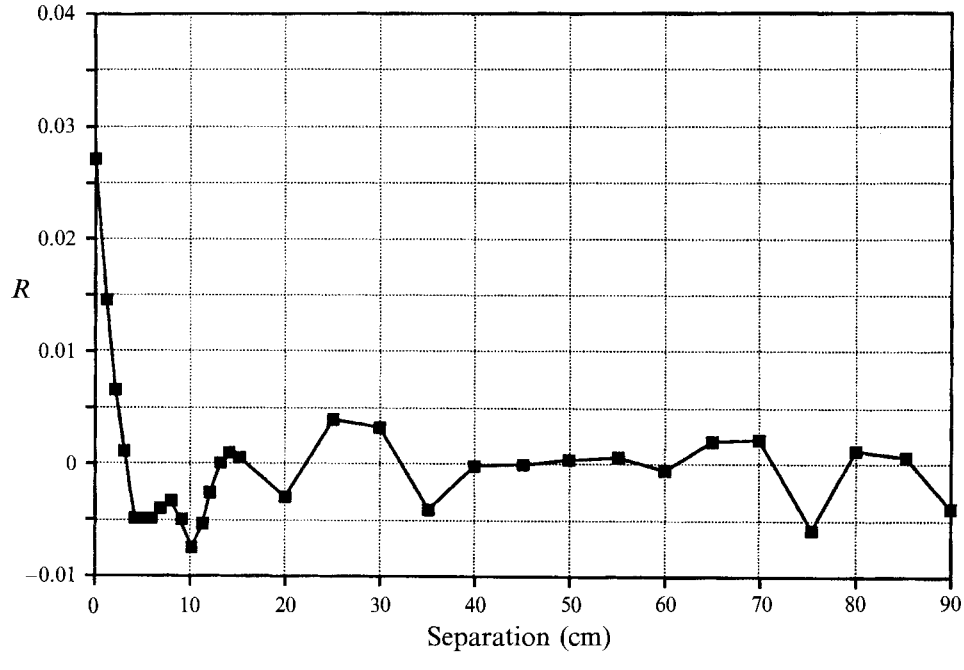

FIGURE 3. Correction function of permeability in the Berea core.

core was set in the vertical position to ensure a one-dimensional displacement, with the lighter fluid injected at the top or the heavier fluid injected at the bottom.

To determine the dispersivity of the core, we conducted a series of five water/brine displacement experiments in which M was close to 1 and N_G varied from almost zero

	Property	Value			
		Water	Brine	Gas	Oil
C	concentration (% NaCl)	0.5	10	—	—
x	mole fraction methane	—	—	0.75	—
	propane	—	—	0.25	—
	n-decane	—	—	—	1.00
ρ	density (kg m^{-3})	993	1059	250	709
μ	viscosity (mPa s)	0.48	0.58	0.030	0.65
D	diffusion coefficient (m^2 s^{-1})	3.0×10^{-9}		4.9×10^{-8}	

TABLE 2. Properties of water and brine at 10.0 MPa and 55 °C and of gas and oil at 25.0 MPa and 60 °C

(0.066) to 1.05. N_G was varied to make it possible to find the dispersivity from the measurements by extrapolation of the measured dispersion when N_G tends to 0. The brine (which had a (high) NaCl concentration of 10% wt) differed a little in viscosity and a density from the water (which did not have a zero NaCl concentration but a low one of 0.5% wt to prevent permeability impairment). The mobility ratio was 1.21 or 0.83 (depending on the displacement direction). In view of the observation of Brigham *et al.* (1961) in an experiment with $M = 0.175$, we judged the values of 0.83 and 1.21 to be sufficiently close to 1 to expect just a small effect from the viscosity contrast. Properties of the water and brine are listed in table 2.

To investigate the effect of gravity number at $M \gg 1$, we conducted three gas/oil displacements with $M = 22$. The displacement direction was downwards with the gas on top of the oil. In this series of experiments, the gravity number varied from 1.9 to a (large) value of 12, the latter for extrapolation to infinite N_G (corresponding to zero displacement velocity). We used a mixture of methane (mole fraction 0.75) and propane as the gas, and n-decane as the oil. The properties are listed in table 2.

In both the water/brine and the gas/oil displacements, the effluent density, measured at regular intervals of 5 or 10 minutes, was converted to concentration using standard correlations. The resulting plots of concentration are shown in figure 4. A match was made between concentration and equation (12) by linear regression. The resulting values of the dispersion K_e are listed in table 3, together with the value of the correlation coefficient of the linear regression. To check the value of the dispersion coefficient, C was calculated with equation (12) and was plotted in figure 4 for comparison with the C values from the measurements.

The convective dispersion K_c was isolated from the total dispersion K_e by subtraction of the dispersion K_{tube} in the inlet and outlet tubes (dead volume) and of the molecular diffusion term. The dispersion in the inlet and outlet tubes was determined by additional displacement experiments in which the core was bypassed, and appeared to be small (about 1% of the total dispersion). The molecular diffusion term $D/F_R\phi$ was determined from measured values of F_R and ϕ and empirical correlations (Chang & Myerson 1985; Renner 1986) for the diffusion coefficient D. For the gas/oil experiments, the value of D was not accurate enough in view of the small convective dispersion at high N_G values, and therefore $D/F_R\phi$ was determined by equating this term to $K_c + D/F_R\phi$ at $N_G = 12$, where the convective dispersion K_c is practically zero according to (11) (small U).

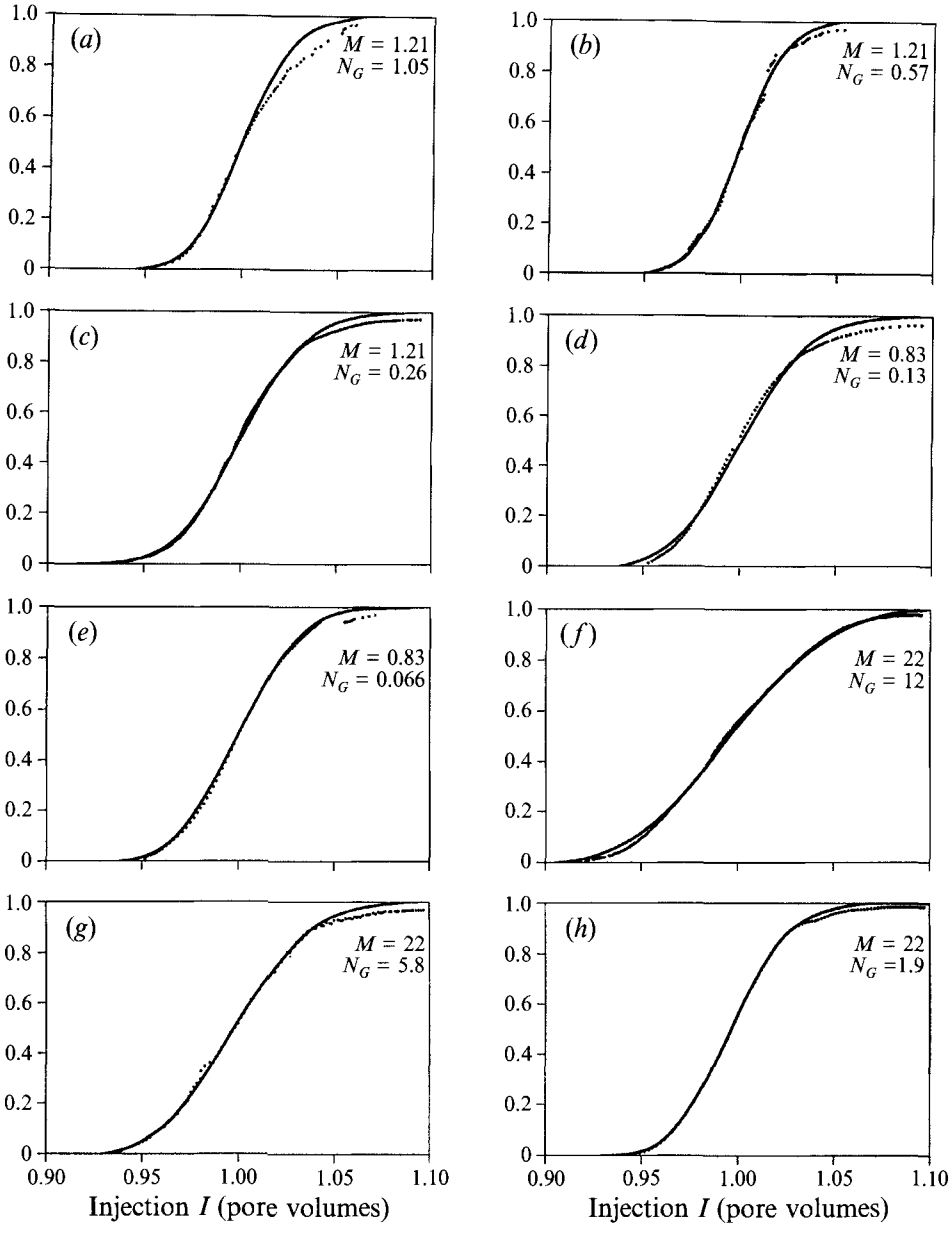

FIGURE 4. Concentration of displacing fluid in effluent versus dimensionless time: ——, matched; · · · · · ·, measured. (*a–e*) water/brine; (*f–h*) gas/oil. Every third point is plotted in (*a*).

3.3. *Effect of small density contrast*

Experiments Ac, Ad and Ae obey the simple model: convective dispersion is proportional to displacement velocity. The proportionally constant is equal to the effective dispersivity without the effect of gravity and thus, since the mobility ratio is close to 1, is roughly equal to the dispersivity β_0 of the core. We denote this dispersivity as β_{ref}. The value of β_{ref}, determined in this way, is $6.3 \pm 0.6 \times 10^{-4}$ m. This value is in agreement within the error bounds with the value of β_0 determined from the mini-permeameter measurements.

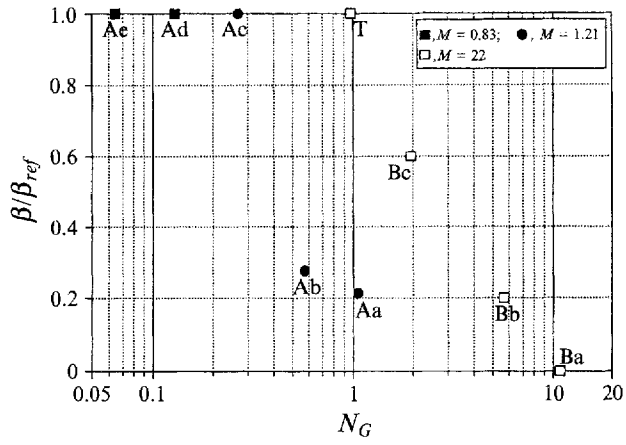

FIGURE 5. Dispersivity ratio β/β_{ref} as a function of gravity number of water/brine and gas/oil displacements (see table 3).

Exp. number	U (m s^{-1})	M	N_G	$K_e - K_{tube}$ (m^2 s^{-1})	N	R^2	β/L	β/β_{ref}	α_e	α_m	$\alpha_e - \alpha_m$
Aa	2.06×10^{-6}	1.21	1.05	8.0×10^{-10}	71	0.9959†	0.73×10^{-4}	0.21	0.17	0.44	−0.27
Ab	3.70×10^{-6}	1.21	0.57	1.18×10^{-9}	55	0.9954	0.98×10^{-4}	0.28	0.23	0.68	−0.45
Ac	8.24×10^{-6}	1.21	0.26	5.70×10^{-9}	286	0.9981	3.44×10^{-4}	0.99	0.79	0.92	−0.13
Ad	2.00×10^{-5}	0.83	0.13	1.30×10^{-8}	59	0.9948	3.45×10^{-4}	0.99	0.79	0.77	0.02
Ae‡	3.94×10^{-5}	0.83	0.066	2.55×10^{-8}	54	0.9997	3.47×10^{-4}	1.00	—	0.80	—
Ba‖	1.50×10^{-6}	22	12.0	2.26×10^{-9}	194	0.9986	0	0	—	0	—
Bb	3.00×10^{-6}	22	5.8	2.66×10^{-9}	52	0.9988	0.71×10^{-4}	0.20	0.16	0	0.16
Bc	9.26×10^{-6}	22	1.9	5.76×10^{-9}	38	0.9999	2.07×10^{-4}	0.60	0.47	0.09	0.38

† Match between $C = 0.1$ and $C = 0.65$.
‡ This experiment was used to determine the magnitudes of β_{ref} and α_{ref}.
‖ This experiment was used to determine the magnitude of $D/F_R\phi$.

TABLE 3. Measured dispersion of water/brine (Aa–Ae) and gas/oil (Ba–Bc) displacements, together with a comparison between the dispersivity ratio predicted by the model (α_m) and measured (α_e) (see §5.4). $D/F_R\phi = 5.20\times10^{-10}$ m^2 s^{-1} (water/brine), and 2.26×10^{-9} m^2 s^{-1} (gas/oil); $\beta/L = (K_e - K_{tube} - D/F_R\phi)/UL$; N is the number of data points and R^2 the correlation coefficient. $\alpha_e = (K_e - D/F_R\phi - K_{tube})\,U\,\beta_{ref}/\alpha_{ref}$ ($\alpha_{ref} = 0.80$)

If we plot the ratio β/β_{ref} of the water/brine displacements as a function of gravity number (figure 5), we see that between $N_G = 0.26$ and $N_G = 1.05$ a large decrease in effective dispersivity occurs from about $1.0\beta_{ref}$ to $0.21\beta_{ref}$. Note that although the density difference between water and brine is very small (just 6% of the average density), the effective dispersivity can be much lower (in this case a factor of 5 lower) than the dispersivity of the core. In the framework of similarity groups, particularly with the use of the gravity number, this can now be understood: the effective dispersivity decreases with gravity number and the decrease is largest at N_G between 0.1 and 1, in correspondence with the experiments of Slobod & Howlett (1964).

3.4. *Effect of gravity number at* $M \gg 1$

The ratio between effective dispersivity and dispersivity of the core is plotted for the gas/oil displacements in figure 5 also. Note in this plot the sharp decrease of effective dispersivity with N_G, in this case between $N_G = 1.9$ and $N_G = 5.8$. We have added the

theoretical data point T: $\beta = \beta_0$ at $U = U_c$ (corresponding to $N_G = 1 - 1/M = 0.95$) to figure 5. We can conclude from figure 5 that there is a strong decrease of effective dispersivity with gravity number in the conditionally stable regime ($M > 1$, $N_G > 1 - 1/M$). This decrease occurs between $N_G = 1$ and $N_G = 10$.

3.5. *Amalgamation of all measurements*

Although the porous media were not the same in the various investigations, the results of the measurements are consistent. As a result, we can summarize all measurements discussed in the following list of seven observations:

(i) an increase in effective dispersivity with mobility ratio (at horizontal orientation and $M \leqslant 1$) (Brigham *et al.*; Giordano *et al.*);

(ii) a non-zero effective dispersivity at M close to 0 (horizontal orientation) (Giordano *et al.*);

(iii) an increase in effective dispersivity with displacement velocity ($M < 1$) (Slobod & Howlett; Ben Salah; this work);

(iv) no dependence of effective dispersivity on displacement velocity at high displacement velocity ($M < 1$) (Slobod & Howlett; Newberg & Foh; this work);

(v) no dependence of effective dispersivity on displacement velocity when the densities of the fluids are the same ($M < 1$) (Slobod & Howlett);

(vi) a small density difference between displacing and displaced fluid, such as that between water and brine, suppresses the effective dispersivity significantly if the displacement velocity is sufficiently low (this work);

(vii) a strong increase in effective dispersivity with displacement velocity at high but stable displacement velocities and $M > 1$ (this work).

Translating these seven observations in terms of the similarity groups, gives the following three observations:

(i) an increase in effective dispersivity with M (at $N_G = 0$ and $M \leqslant 1$);

(ii) a non-zero effective dispersivity at M close to 0 (at $N_G = 0$);

(iii) a decrease in effective dispersivity with N_G in the region of $N_G = 1$ (independent of M and $N_G > 1 - 1/M$ if $M > 1$).

4. Numerical simulations to test dispersive behaviour

Because of the concentration dependence of the viscosity μ and the generally nonlinear concentration dependence of the density ρ, the basic equations (1)–(3) are nonlinear in the concentration c. It is therefore not obvious beforehand that the $X^{\frac{1}{2}}$ dependence of the transition zone length in the absence of viscosity and density contrasts also occurs in the presence of these contrasts. To test the dispersive behaviour of the transition zone, i.e. an expansion of the transition zone with $X^{\frac{1}{2}}$, we have carried out numerical simulations of stable, linear, miscible displacements in a wide range of mobility ratios and gravity numbers. The simulations were also used to test our random-walk model (see § 5).

4.1. *Set-up of simulations*

The simulator used incorporates the basic equations (1)–(3) of the flow of incompressible, miscible fluids under gravity (Crump 1988). The numerical scheme of the simulator has second-order truncation error in space and suppresses oscillations (Total Variation Diminishing scheme, see Harten 1984; Yang & Lee 1988).

(*a*)

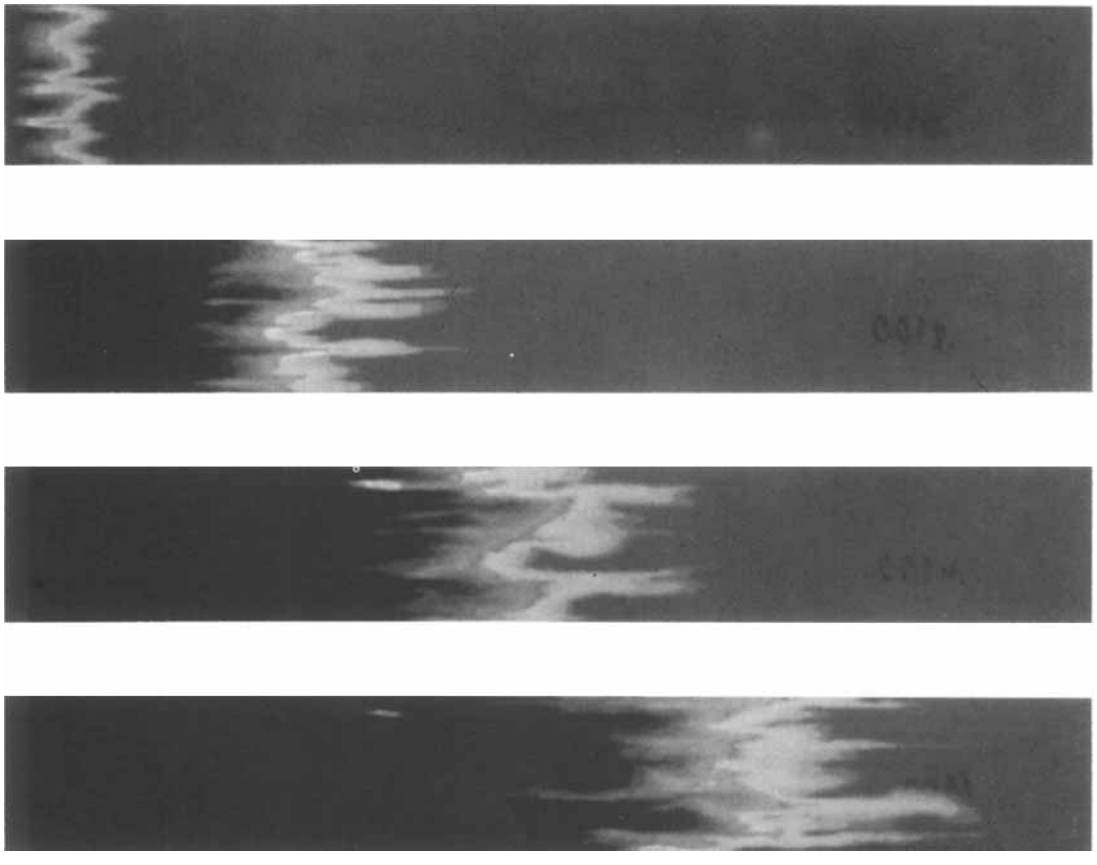

(*b*)

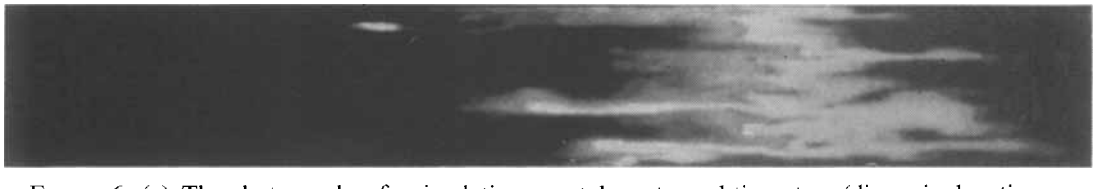

FIGURE 6. (*a*) The photographs of a simulation run, taken at equal time steps (dimensionless times $I = 0.05, 0.25, 0.45, 0.65$), show a stable displacement of a fluid by a more viscous, miscible fluid through a porous medium with a large number of local-scale permeability variations. In can be seen that fingerlike disturbances between the fluids successively grow, split, merge and disappear. After some evaluation of the various stages, it can be demonstrated that the mixing zone between the fluids expands with the square root of the displacement distance. The standard deviation σ of the log-permeability distribution is 0.96 and the displacing fluid is 5 times more viscous than the displaced fluid ($M = 0.2$). (*b*) A picture for the same permeability field as (*a*) at the same time as the bottom picture of (*a*) but for a displacement with no viscosity contrast ($M = 1$). This illustrates a part of the subject of this paper: the suppression of the length of the mixing zone by the viscosity contrast between the fluids.

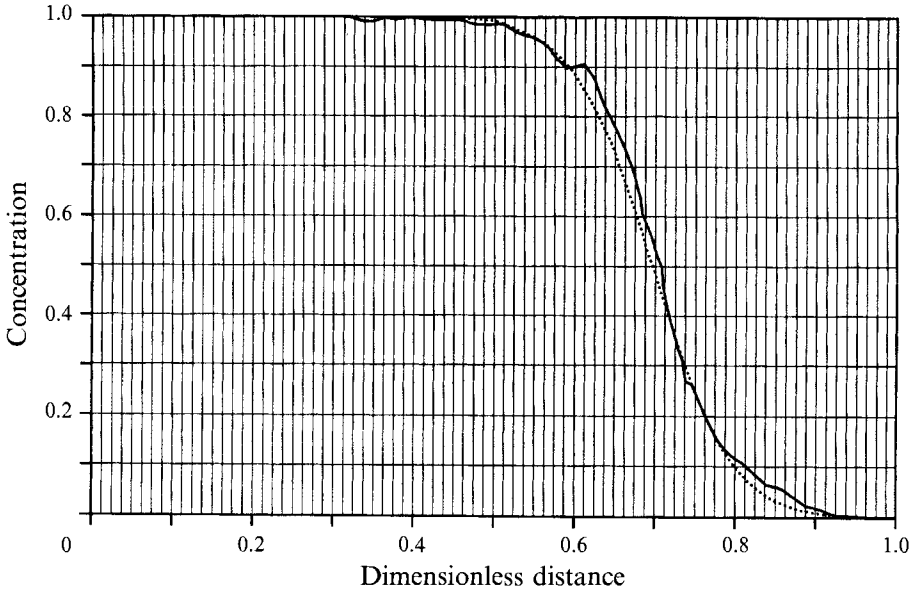

FIGURE 7. Concentration profile at $I = 0.7$ of the run with $\sigma = 0.96$, $M = 0.2$, $N_G = 0$: ——, simulation; · · · · · ·, matched with $\beta/L = 0.0048$.

400 random permeabilities from a log-normal distribution were assigned to a configuration of 20 rectangles by 20 rectangles. The length/width ratio of the rectangles was 6.8. Each rectangle was divided into a fine mesh of 4 × 4 grid blocks. The result was a finely gridded configuration containing 6400 grid blocks. We created two grids, one with a standard deviation σ of the log-permeability distribution equal to 0.96, and another equal to 0.45. In test runs with $M = 1$ and $N_G = 0$ we found that the dispersivity of each grid was in agreement with Gelhar & Axness's theory. We thereby adapted the spatial correlation function used by Gelhar & Axness to account for the correlation function of the grid and for the fact that the simulator uses harmonic weighting of permeabilities for adjacent blocks. The resulting correlation length λ was equal to 0.02 times the total length L of the configuration. The number of 20 rectangles in the flow direction appeared to be sufficient to neglect the presence of the boundaries of the total configuration on the correlation function (Kempers 1991).

4.2. *Evaluation*

After each time interval of $0.01L/U$, a concentration pattern was generated, from which a value of the dispersivity was calculated. This made it possible to monitor the development of the dispersivity over time, which is a distinct advantage compared to the determination of dispersion from the production history as we were forced to do in the core-flooding experiments. An example of four such concentration patterns is shown in figure 6(*a*). The calculation of dispersivity is based on equation (12). To match the concentration patterns with (12), the concentration of the solvent in an array of blocks in the transverse flow direction was averaged.

An example of a concentration profile is plotted in figure 7, showing an S-shaped profile. This profile was matched with (12) from which the dimensionless dispersivity β/L was determined. The correlation coefficient of this match is 0.993. The plot of β/L versus dimensionless time $I = Ut/L$, determined from a series of concentration patterns of this run, is shown in figure 8. The figure indicates that the dispersivity of this

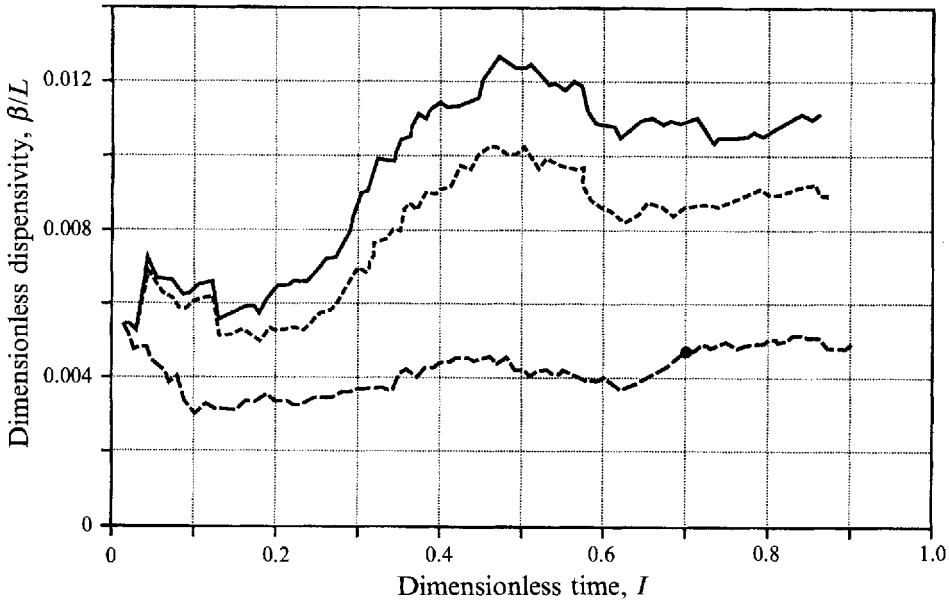

FIGURE 8. Effective dispersivity as a function of time in three simulation runs ($\sigma = 0.96$): ——, $M = 1$, $N_G = 0$; - - -, $M = 2$, $N_G = 0.805$; – – –, $M = 0.2$, $N_G = 0$; ●, an example data point determined from figure 7.

σ	M	N_G	$10^2\beta_s/L$	$10^2\beta_{th}/L$	α_s	α_m	$\alpha_s-\alpha_m$
0.96	1	0	1.12±0.06	0.95	1.000	—	—
0.45	1	0	0.37±0.03	0.357	1.000	—	—
0.96	0.2	0	0.44±0.04	—	0.392±0.043	0.390	0.002
0.96	1	0.135	1.02±0.06	—	0.909±0.100	0.917	−0.008
0.96	0.1	0	0.35±0.03	—	0.313±0.034	0.316	−0.003
0.96	2	0.805	0.91±0.06	—	0.812±0.065	0.801	0.011
0.96	0.01	0	0.29±0.02	—	0.259±0.021	0.255	0.004
0.96	10	1.347	0.76±0.08	—	0.677±0.088	0.688	−0.011
0.45	0.1	0	0.117±0.006	—	0.315±0.028	0.309	0.006
0.45	10	1.384	0.177±0.007	—	0.475±0.038	0.499	−0.024
0.96	0.5	0	0.66±0.05	—	0.588±0.058	0.631	−0.043
0.96	1	1.409	0.56±0.06	—	0.496±0.055	0.453	0.043
0.96	0.1	13.41	0.20±0.02	—	0.180±0.022	0.134	0.046
0.96	10	2.683	0.36±0.05	—	0.320±0.051	0.235	0.085
0.96	2	5.634	0.21±0.01	—	0.184±0.015	0.060	0.124
0.96	10	5.365	0.24±0.01	—	0.212±0.015	0.026	0.186

TABLE 4. Effective dispersivity and its variation in simulation runs, together with a comparison between the model (see §5) and the simulation runs. Subscript s refers to simulation result; subscript th refers to prediction by the theory of Gelhar & Axness; subscript m refers to the model (see §5).

run (and of two other runs) does not fluctuate very much with I apart from a transient for values of I below about 0.35. (The transient is caused by the forced uniform injection and the fact that the displacement front has travelled through too few heterogeneities to be dispersive.) For such a curve (without the transient) an average value of β/L can be calculated yielding a small standard deviation if the transition zone is dispersive.

In addition to two reference runs for $M = 1$ and $N_G = 0$, we conducted fourteen simulation runs for a wide range of M and N_G values (M between 0.01 and 10; N_G between 0 and 10). The correlation coefficient of the match between the concentration profile and the theoretical expression (12) for the concentration was higher than 0.99 in all runs. We observed dispersive behaviour of the transition zone in all runs. This is illustrated by the small standard deviation of the average β/L values (10% or smaller as in the reference runs, see table 4).

To isolate the effects of the fluid properties on the dispersivity we define a dispersivity ratio α:

$$\beta = \alpha\beta_0. \tag{18}$$

By definition α lies between 0 and 1. The table shows that the effect of the density and viscosity contrast can be significant. The α values confirm the three qualitative observations derived from the experiments (§3.5).

5. Random-walk model for the magnitude of the dispersivity

One model has been reported that claims to quantify the dispersivity in the presence of a viscosity difference. This model, reported in Heinemann & Munka (1983), is a synthesis of previous models, but lacks a derivation. Many assumptions underlie the model and it contains four matching parameters, hence predictive power is very limited.

We present a model without matching parameters. It makes use of a random-walk concept for the different parts of the displacement front, which enables us to calculate the dispersion coefficient as a function of the step size in the random-walk process. We show a way to calculate the step size and we demonstrate that the resulting expression for the dispersion coefficient reduces to the expression derived by Gelhar & Axness if no density contrast and no viscosity contrast are present. The model is tested against the core-flooding experiments and numerical simulations presented above.

5.1. *Development of model*

Here, we present a short outline of the model; a more elaborate treatment can be found in Kempers (1991). Like Gelhar & Axness, we assume that the permeability is distributed randomly in all directions and has a log-normal frequency distribution and a small correlation length compared to the system length. Furthermore, we assume that the displacement occurs in one of the three eigen directions of the permeability tensor; for example, displacement parallel to the bedding. Another assumption is that at least one of the two correlation lengths perpendicular to the flow direction is small compared with the correlation length in the flow direction. This assumption is satisfied in layered depositions with a layer thickness which is small compared with the correlation length in the flow direction. Furthermore, we assume that molecular diffusion is negligible.

Like Scheidegger (1957), we assume that different parts of the displacement front undergo a linear displacement (in each time step τ a displacement Λ_0; velocity $U = \Lambda_0/\tau$) with a random-walk process (with step size $\Lambda_0\sigma_\Lambda$) superimposed. We then have

$$K = \frac{1}{2}\frac{(\text{step size})^2}{\text{time step}} = \tfrac{1}{2}U\Lambda_0\sigma_\Lambda^2 \tag{19}$$

for the dispersion coefficient (Scheidegger 1957). Scheidegger did not, however, relate the statistical parameters σ_Λ and Λ_0 to properties of the porous medium. We added a new element to the Scheidegger theory: we related the step size in the random-

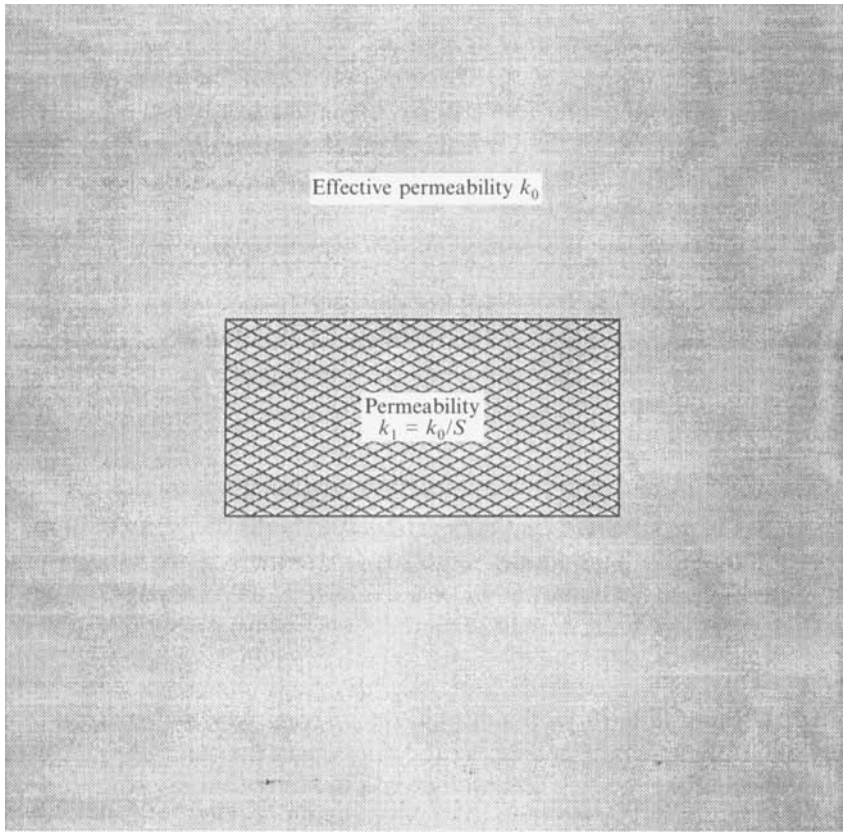

FIGURE 9. Reservoir block of different permeability surrounded by an infinite medium with effective permeability.

walk process to properties of the porous medium using the simple fact that in every time step each part of the displacement front travels a distance that is proportional to the local permeability. For simplicity we considered the permeability as constant over this distance; the permeability is of random value and does not correlate with adjacent permeability values.

To quantify the statistical parameters σ_A and A one rectangular block of distinct permeability k_1 is selected from the heterogeneous porous medium. We consider this block as embedded in an infinite, homogeneous porous medium with effective permeability k_0 (see figure 9). The block length is A_0; it can be simply shown that half this length corresponds to the longitudinal correlation length of the permeability, λ. The widths of the block are related similarly to the transverse correlation lengths λ' of the permeability. Figure 10 shows the distortion of the displacement front as it traverses the configuration of figure 9. (In reality, the distortion is different at the lateral boundaries of the block, but this has been neglected, see § 5.3). A calculation of the location A_1 of the displacement front between the fluids should be carried out for an ensemble of configurations as in figure 9, each with one block of permeability k_1, the value of which is randomly taken from the permeability frequency distribution. However, it was then found that no closed analytical expression for A_1 as a function of k_1, could be calculated. This prohibits a direct calculation of the dispersion coefficient, K. Therefore, we assumed that the effect of the nonlinearity in (1)–(3) is weak, which means that the distribution of A values is the same as that of the

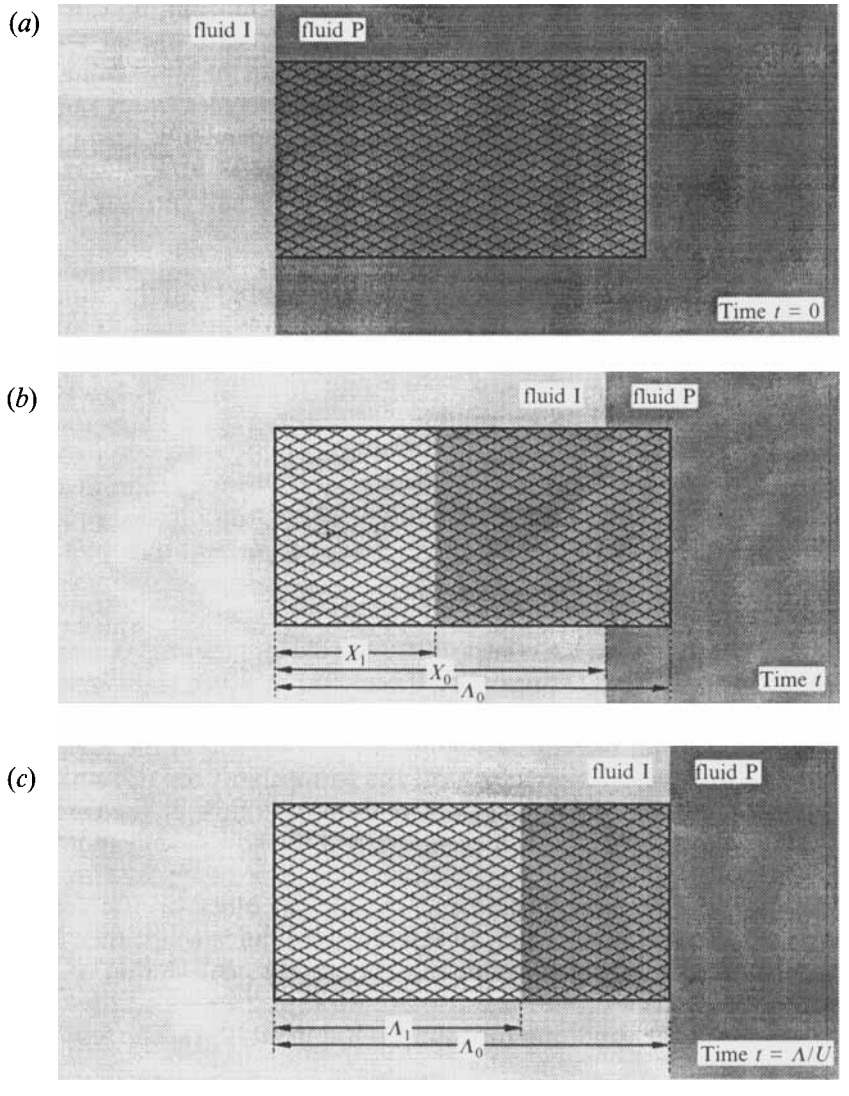

FIGURE 10. Position of displacement front between injected fluid I and produced fluid P according to random-walk model.

permeabilities k. Note that this assumption is sustained by the good match found between (12) and the numerical simulations. As a result, Λ_1 has to be determined only once: for the case that the log-permeability of the selected block differs from the log-permeability of the surrounding medium by the standard deviation σ, corresponding to $k_0/k_1 = e^{\sigma} = S$, where S is the geometrical standard deviation of the permeability distribution. The standard deviation σ_Λ is thus given by

$$\sigma_\Lambda = \ln(\Lambda_0/\Lambda_1). \tag{20}$$

The proposed expression for the effective dispersivity is, with substitution of (20) in (19) and of $\lambda = \frac{1}{2}\Lambda_0$:

$$\beta = K/U = \lambda[\ln(\Lambda_0/\Lambda_1)]^2. \tag{21}$$

Substitution of (11) and (18) in (21) gives the following expression for the dispersivity ratio α:

$$\alpha = \beta/\beta_0 = [\ln(\Lambda_0/\Lambda_1)]^2/\sigma^2. \tag{22}$$

The equation of motion for the location of the displacement front, A_1, can be restricted to one dimension, because of the assumption that at least one of the transverse correlation lengths of the permeability is much smaller than the longitudinal correlation length. The one-dimensional equation of motion, which includes Darcy and hydrostatic pressure terms, and its solution of A_1 are listed in the Appendix. If fluid properties are not taken into account, it can be simply shown that $A_0/A_1 = k_0/k_1$. Then (21) reduces to Gelhar & Axness's expression (11) (apart from their small correction factor).

5.2. *Results*

We present the results of the Appendix graphically: in figure 11(*a*) the dispersivity ratio α, is plotted as a function of gravity number N_G, with mobility ratio M and geometric standard deviation S as parameters. For the special case of a vanishing displacement velocity, gravity forces dominate over viscous forces. In equation (A 1) all Darcy terms vanish and the solution is $x_0 = x_1$, resulting in $\alpha = 0$. Figure 11(*b*) shows another special case: the dispersivity ratio as a function of mobility ratio when gravity has no effect (zero gravity number). Figure 11(*c*) shows the dispersivity ratio as a function of gravity number in a third special case, that of mobility ratio equal to 1. In displacements of fluids with about equal fluid properties, this plot is a good approximation.

5.3. *Deviation*

The model clearly demonstrates a contrast between the longitudinal velocity inside and outside the block of different permeability. There are, however, transverse flow effects which we have not incorporated in our one-dimensional equation of motion. These effects are generally small but can be important. It is present in the following cases.

(*a*) Both transverse correlation lengths of the permeability are not small compared with the longitudinal correlation length. The transverse flow at the entrance of the block of deviating permeability is not negligible and the flow field cannot be modelled as one-dimensional.

(*b*) At small α, the pressures inside and outside the block are far from being in equilibrium at the lateral boundaries. In this case, the fluids adapt their longitudinal velocity significantly to restore pressure equilibrium. The calculation of A_1 does not take account of this effect.

We have estimated the condition for case (*a*) (Kempers 1991). The result is that this case can be neglected if

$$\lambda'/\lambda\,(1-1/S) \ll 1, \tag{23}$$

in which the smallest of the two transverse correlation length should be used for λ'. For example, in our numerical simulations with $\sigma = 0.96$ and $\sigma = 0.45$ the left-hand side of (23) is equal to 0.09 and 0.05 respectively and thus (23) is satisfied.

5.4. *Comparison to core-flooding experiments*

It can be easily checked that the three observations that were derived from the core-flooding experiments agree with the random-walk model. A quantitative comparison between model and measurements of effective dispersivity is not possible for the measurements reported in the literature, as λ and σ were not reported. However, we measured the permeability field of the Berea core and could therefore determine λ and σ.

In table 3 the experimental value α_e and the model prediction α_m are also listed for both the water/brine and the gas/oil displacements in the Berea core. Experiment Ba, which was used to determine $D/F_R\phi$ for the gas/oil displacements, is listed in the table but is not used for the comparison between experiments and model. Table 5 shows that

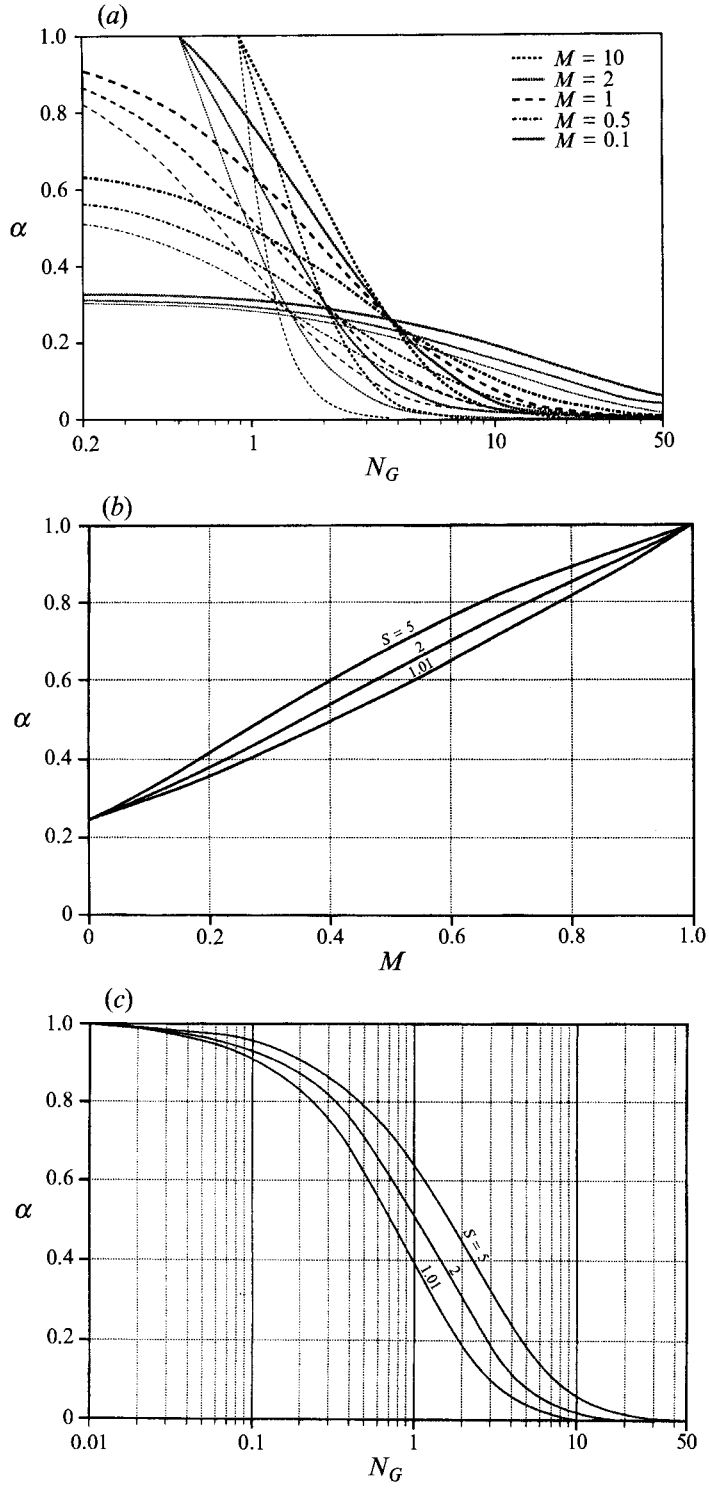

FIGURE 11. (*a*) Dispersivity ratio α as a function of gravity number N_G with parameters mobility ratio M and geometrical standard deviation S (thinnest curves, $S = 1.01$; middle curves, $S = 2$; thickest curves, $S = 5$). (*b*) α as a function of M at $N_G = 0$ (parameter S). (*c*) α as a function of N_G at $M = 1$ (parameter S).

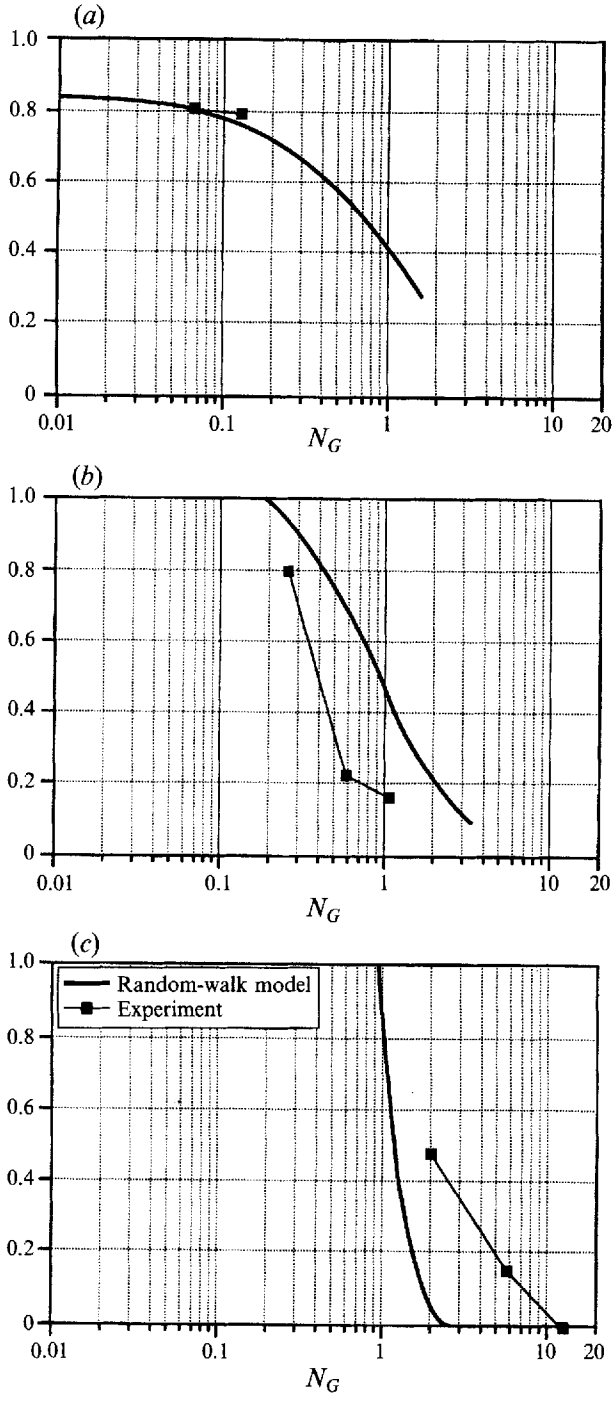

FIGURE 12. Comparison between random-walk model and experiments in Berea core. (*a*) $M = 0.83$, (*b*) $M = 1.21$, (*c*) $M = 22$. ——, random-walk model (α_m); —■—, experiment (α_e).

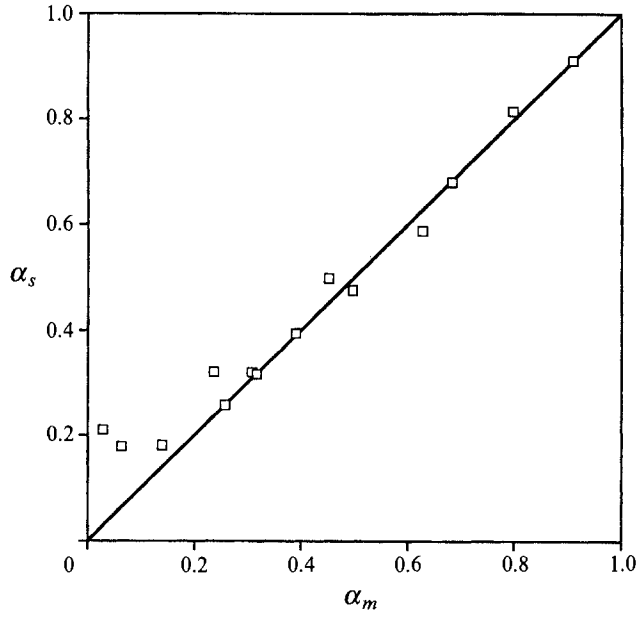

FIGURE 13. Comparison between dispersivity ratio α_m predicted by random-walk model and dispersivity ratio α_s determined from simulation runs.

three of the six α_e values agree within 0.16 with the model prediction; the other three α_e values differ up to 0.45 from the model prediction. The large deviation of these three values from the model prediction may be an effect of the transverse correlation length which is probably not much smaller than, but about equal to, the longitudinal correlation length. The left-hand side of (23) gives 0.16 in this case. Furthermore, for experiment Bc α is very sensitive to N_G. For example, a decrease of N_G from the present value 1.9 to 1.26 results in a drastic increase of α from the present value 0.09 to the measured value 0.47.

In figure 12 we have plotted α_e and α_m against N_G for comparison. The figure shows that, although the quantitative test of the model is not fully convincing, the experiments in the Berea core all agree qualitatively with the random-walk model.

5.5. *Comparison to numerical simulations*

The dispersivity ratio α_s of a simulation run was calculated from the average β/L value of the simulation run and the average β/L value of the reference run. Table 4 lists the calculated α_s values (and their error due to the fluctuation of β/L as a function of I) and the α_m values predicted by our model.

For ten runs our model predicts an α value that agrees with α_s within the error bounds. Figure 13 shows that of the fourteen data points all but two are close to the ideal line $\alpha_s = \alpha_m$, illustrating the good quantitative agreement for these data points. The figure also shows that the data points that deviate most widely from the ideal line $\alpha_s = \alpha_m$ have a small α_m value (below 0.15). The α_s value stabilizes at a more or less constant value of 0.20, while the α_m value goes to zero. A possible explanation for the deviation between the two α values at small α_m is the transverse flow effect that has been discussed in §5.3. This phenomenon occurs particularly at small α_m and is not included in the model. The deviation between the two α values at small α_m can be partly explained by the contribution from the numerical dispersion (which corresponds to $\alpha_s = 0.01$).

6. An example

As an illustration of our work, we consider the oil recovery project in the Westpem Nisku D Reef in Canada, in which oil is displaced by miscible gas. Da Sie & Guo (1990) evaluated the performance of this flood, which was conducted vertically. One of their three conclusions is that the observed mixing zone between the solvent and the oil is 'much smaller (< 8.5 m) than expected'. The authors' explanation is: 'dispersion of the solvent into the oil is probably not significant in a scheme where gravity segregation of gas and oil dominates flood mechanics'. We show below that our model predicts a very small mixing zone length due to gravity segregation, thus providing a basis for their explanation.

The flood started in May 1981. The displacement velocity of the flood is low: in December 1986 the solvent/oil interface was at a depth of 2129.5 m and in May 1987, it had reached a depth of 2130.6 m, so the displacement velocity at that time was $2130.6-2129.5 = 1.1$ m per 5 months or 8.5×10^{-8} m s^{-1}. With fluid and rock data from Da Sie & Guo ($\mu_{oil} = 0.19$ mPa s, $\mu_{solvent} = 0.026$ mPa s, $\rho_{oil} = 540$ kg m^{-3}, $\rho_{solvent} = 210$ kg m^{-3}, $k_{vertical} = 0.110$ μm^2, $\phi = 0.12$) we can calculate two important parameters: mobility ratio M is 7.3 and gravity number N_G is 180. This shows that the flood is indeed extremely gravity-dominated.

Figure 11(*a*) can be used to find the dispersivity ratio α at these parameter values. Interpolation between the $M = 2$ and the $M = 10$ curves in figure 11(*a*) to find α at $M = 7.3$, shows that α is practically zero at N_G larger than 50. Da Sie & Guo do not provide information about the permeability variation but this is no problem, because α is practically zero for a wide range of S values (between 1 and 5 at least). So at $N_G = 180$, α has such a low value that macroscopic dispersion is negligible in this flood.

Because the macroscopic dispersion is suppressed, we expect the dispersion zone to be dominated by molecular diffusion (microscopic convective dispersion is negligible because of the very low displacement velocity). For example, with a guessed value $D/F_R\phi = 10^{-9}$ m^2 s^{-1}, the dispersion zone length in May 1987 (after starting in May 1981) is about $3.62\ \{10^{-9}\ \text{m}^2\ \text{s}^{-1}\times 6\ \text{years}\}^{\frac{1}{2}} = 1.8$ m. This value agrees with the observation that the dispersion zone length is smaller than the distance between two sampling points, which was 8.5 m.

7. Conclusions

(i) Dispersivity is not solely a property of the porous medium in cases where the fluids differ in density and/or in viscosity. Dispersivity should be seen as an effective property that also takes fluid dynamics into account.

(ii) We have made a coherent evaluation of the measurements of effective dispersivity in stable, miscible displacements conducted with a wide variety of porous media and fluids in terms of dimensionless similarity groups (gravity number N_G and mobility ratio M).

(iii) Our core-flooding experiments and detailed numerical simulations have shown good matches between the error function and the concentration profiles, thus indicating that the transition zone does expand with $X^{\frac{1}{2}}$ in the presence of a density contrast and/or a viscosity contrast between the fluids; a strong dependence of effective dispersivity on displacement velocity in the conditionally stable regime; that a very small density difference, such as that between water and brine, can suppress the dispersion zone length significantly.

(iv) We have extended the results of random-walk theory with fluid dynamics to

quantify the length of a dispersive transition zone in the presence of a density contrast and a viscosity contrast. (The new model adds to the old relation (11) relation (18) and figure 11.) The three qualitative observations that have been derived from the core-flooding experiments agree with the model. The model prediction of the dispersivity agrees with the dispersivity determined in the simulation runs, except at small dispersivity ratio. This deviation is attributed to a transverse flow effect, which is not incorporated in the model.

The authors are indebted to Professor Dr J. Hagoort for many useful suggestions, to H. K. Groeneweg and M. F. J. van Rijen for their respective contributions to the core-flooding experiments and the numerical simulations, and to the management of Shell Internationale Research Maatschappij BV for permission to publish this paper.

Appendix

The following equations of motion with Darcy pressure drops and hydrostatic pressures apply to the location x_0 of the displacement front inside, and the location x_1 outside, the block with permeability k_1 (see figure 10):

$$\Delta p = \frac{\mu_I}{k_0}\phi\frac{\mathrm{d}x_0}{\mathrm{d}t}x_0+\frac{\mu_P}{k_0}\phi\frac{\mathrm{d}x_0}{\mathrm{d}t}(\Lambda_0-x_0)-\rho_I g x_0\sin\theta-\rho_P g(\Lambda_0-x_0)\sin\theta$$

$$= \frac{\mu_I}{k_1}\phi\frac{\mathrm{d}x_1}{\mathrm{d}t}x_1+\frac{\mu_P}{k_1}\phi\frac{\mathrm{d}x_1}{\mathrm{d}t}(\Lambda_0-x_1)-\rho_I g x_1\sin\theta-\rho_P g(\Lambda_0-x_1)\sin\theta \qquad \text{(A 1)}$$

with boundary conditions:

$$\text{at } t=0,\quad x_1=0;\quad \text{at } t=\Lambda_0/U,\quad x_1=\Lambda_1;\quad x_0=Ut.$$

We define

$$\omega = S\frac{1-1/M}{N_G}[(1-M)\Lambda_1/\Lambda_0+M]-\tfrac{1}{2},$$

$$\omega_0 = S\frac{1-1/M}{N_G}-\tfrac{1}{2},\quad a = S\frac{1-1/M}{N_G}\left(1-\frac{1-1/M}{N_G}\right)-\tfrac{1}{4}.$$

The solution to the differential equation (A 1) is the following set of implicit equations depending on the sign of a (for derivation see Kempers 1991):

$$\left.\begin{aligned}
&\text{if } a>0:\quad 0=-\ln M+\tfrac{1}{2}\ln\left(\frac{\omega^2+a}{\omega_0^2+a}\right)+\frac{1}{2a^{\frac{1}{2}}}\arctan\left(\frac{a^{\frac{1}{2}}(\omega-\omega_0)}{a+\omega\omega_0}\right),\\
&\text{if } a=0:\quad 0=-\ln M+\ln\frac{|\omega|}{|\omega_0|}-\frac{1}{2\omega}+\frac{1}{2\omega_0},\\
&\text{if } a<0:\quad 0=-\ln M+\left[\frac{1}{2}+\frac{1}{4(-a)^{\frac{1}{2}}}\right]\ln\left(\frac{|\omega^2+a|}{|\omega_0^2+a|}\right)+\frac{1}{2(-a)^{\frac{1}{2}}}\ln\left(\frac{\omega_0+(-a)^{\frac{1}{2}}}{\omega+(-a)^{\frac{1}{2}}}\right).
\end{aligned}\right\} \qquad \text{(A 2)}$$

To find Λ_1, the equations have to be solved numerically. The number of roots is 1 at maximum in the interval $[0, \Lambda_0]$.

REFERENCES

BEAR, J. & VERRUIJT, A. 1987 *Modeling Groundwater Flow and Pollution.* Reidel.

BEN SALAH, M. D. 1965 Influence des contrastes de viscosité et de densité sur le déplacement en milieu poreux de deux fluides miscibles. *Rev. l'Inst. Français Pétrole* **20**, 1237–1255.

BRIGHAM, W. E., REED, P. W. & DEW, J. N. 1961 Experiments on mixing during miscible displacement in porous media. *Soc. Petrol. Engng J.* March 1961, 1–8.

CHANG, Y. C. & MYERSON, A. S. 1985 The diffusivity of potassium chlorides and sodium chloride in concentrated, saturated and supersaturated aqueous solutions. *AIChE J.* **31** (6).

COLLINS, R. E. 1976 *Flow of Fluids through Porous Materials.* Tulsa: Petroleum Publishing Co.

CRUMP, J. G. 1988 Detailed simulations of the effects of process parameters on adverse mobility ratio displacements. *SPE Paper* 17337.

DAGAN, G. 1989 *Flow and Transport in Porous Formations.* Springer.

DA SIE, W. J. & GUO, D. S. 1990 Assessment of a vertical hydrocarbon miscible flood in the Westpem Nisku D Reef. *SPE Res. Engng*, May 1990, 147–154.

GELHAR, L. W. 1986 Stochastic subsurface hydrology from theory to applications. *Water Resour. Res.* **22**, 135S–145S.

GELHAR, L. W. 1988 Stochastic analysis of large scale transport processes. Presented at *Gordon Research Conf. Modelling flow in permeable media, Plymouth, New Hampshire, August 15–19, 1988.*

GELHAR, L. W. & AXNESS, C. L. 1983 Three-dimensional stochastic analysis of macrodispersion in aquifers. *Water Resour. Res.* **19**, 161–180.

GIORDANO, R. M., SALTER, S. J. & MOHANTY, K. K. 1985 The effects of permeability variations on flow in porous media. *SPE Paper* 14365.

HARTEN, A. 1984 On a class of high-resolution total-variation-stable finite-difference schemes. *SIAM J. Numer. Anal.* **21**, 1–23.

HEINEMANN, Z. & MUNKA, M. 1983 The dispersion of miscible fluids with different viscosities in a porous medium. *Erdöl Erdgas* **36**, 300–307.

KEMPERS, L. J. T. M. 1990 Dispersive mixing in unstable displacement. In *Proc. 2nd European Conf. on the Mathematics of Oil Recovery, Arles* (ed. D. Guérillot & O. Guillon), pp. 197–204. Éditions Technip, Paris (*SPE Paper* 22197).

KEMPERS, L. J. T. M. 1991 Dispersive mixing in stable and unstable miscible displacements. Doctoral thesis, Technical University of Delft.

KEMPERS, L. J. T. M. 1992 Effect of fluid properties on convective dispersion: comparison of analytical model with numerical simulations. In *The Mathematics of Oil Recovery* (ed. P. R. King), pp. 775–784. Clarendon.

KEMPERS, L. J. T. M., HAAS, H. & GROENEWEG, H. K. 1992 Experimental observations on dispersive mixing zones in the presence of a viscosity contrast and a density contrast. In *Heat and Mass Transfer in Porous Media* (ed. M. Quintard & M. Todorovic), pp. 525–536. Elsevier.

NEWBERG, M. A. & FOH, S. E. 1988 Measurement of longitudinal dispersion coefficients for gas flowing through porous media. *SPE Paper* 17731.

PERKINS, T. K. & JOHNSTON, O. C. 1963 A review of diffusion and dispersion in porous media. *Soc. Petrol. Engng J.* March 1963, 70–84.

RENNER, T. A. 1986 Measurements and correlation of diffusion coefficients for CO_2 and rich-gas applications. *SPE Paper* 15391.

SCHEIDEGGER, A. E. 1957 *The Physics of Flow through Porous Media.* University of Toronto Press.

SLOBOD, R. L. & HOWLETT, W. E. 1964 Effects of gravity segregation in laboratory studies of miscible displacement in vertical unconsolidated porous media. *Soc. Petrol. Engng J.* March 1964, 1–8.

STALKUP, F. I. 1983 *Miscible Displacement.* SPE Monograph series, vol. 8. Henny L. Doherty Series.

TAYLOR, G. I. 1953 Dispersion of soluble matter in solvent flowing slowly through a tube. *Proc. R. Soc. Lond.* A **219**, 186–203.

WARREN, J. E. & SKIBA, F. F. 1964 Macroscopic dispersion. *Soc. Petrol. Engng J.* September 1964, 215–230.

YANG, J. Y. & LEE, Y. J. 1988 A comparative study of TVB, TVD and ENO schemes for the Euler equations. In *Recent Advances in Computational Fluid Dynamics* (ed. S. A. Orszag & W. Shyy). Springer.